The American Journal of Pathology, Vol. 181, No. 2, August 2012
Copyright © 2012 American Society for Investigative Pathology.
Published by Elsevier Inc. All rights reserved.
http://dx.doi.org/10.1016/j.ajpath.2012.04.023

Molecular Pathogenesis of Genetic and Inherited Diseases

Defective T-Lymphocyte Migration to Muscles in Dystrophin-Deficient Mice

Cynthia M. Cascabulho, Cristiane Bani Corrêa, Vinícius Cotta-de-Almeida, and Andrea Henriques-Pons

From the Laboratory for Innovations in Therapy, Teaching and Bioproducts, Oswaldo Cruz Institute-Fiocruz, Rio de Janeiro, Brazil

Duchenne muscular dystrophy (DMD), an X-linked recessive disorder affecting 1 in 3500 males, is caused by mutations in the dystrophin gene. DMD leads to degeneration of skeletal and cardiac muscles and to chronic inflammation. The *mdx/mdx* mouse has been widely used to study DMD; this model mimics most characteristics of the disease, including low numbers of T cells in damaged muscles. In this study, we aimed to assess migration of T cells to the heart and to identify any alterations in adhesion molecules that could possibly modulate this process. In 6-week-old *mdx/mdx* mice, blood leukocytes, including T cells, were CD62L$^+$, but by 12 weeks of age down-modulation was evident, with only approximately 40% of T cells retaining this molecule. Our *in vitro* and *in vivo* results point to a P2X7-dependent shedding of CD62L (with high levels in the serum), which in 12-week-old *mdx/mdx* mice reduces blood T cell competence to adhere to cardiac vessels *in vitro* and to reach cardiac tissue *in vivo*, even after *Trypanosoma cruzi* infection, a known inducer of lymphoid myocarditis. In *mdx/mdx* mice treated with Brilliant Blue G, a P2X7 blocker, these blood lymphocytes retained CD62L and were capable of migrating to the heart. These results provide new insights into the mechanisms of inflammatory infiltration and immune regulation in DMD. ***(Am J Pathol 2012, 181: 593–604; http://dx.doi.org/10.1016/j.ajpath.2012.04.023)***

Duchenne muscular dystrophy (DMD) is an X-linked recessive disorder that affects 1 in 3500 males and is caused by mutations in *DMD*, the dystrophin gene. *DMD* is the largest gene described in humans, with more than 2.5 million base pairs.[1] The dystrophin protein provides a link between intracellular F-actin and the dystrophin glycoprotein complex (DGC), which binds to laminin in the extracellular matrix.[2] The absence of functional dystrophin destabilizes the muscle fiber, leading to progressive cell damage through membrane leakage.[3] DMD patients are usually wheelchair-bound by 12 years of age and die of cardiac-respiratory failure in their early twenties.[4,5]

The *mdx/mdx* mouse is widely used as an experimental animal model to study DMD. These mice are derived from a naturally occurring mutant that arose within a C57BL/10 colony and were initially defined by high plasma levels of creatine kinase (CK). Although *mdx/mdx* mice have muscle fiber damage and local inflammatory response in muscles, they exhibit only a mild myopathy.[6]

It is postulated that the local inflammatory response in human patients and experimental models further damage the sarcolemma, leading to more myofiber death.[7,8] Cellular inflammatory infiltration in DMD is characterized by high numbers of myeloid cells (mostly macrophages, but also mast cells and others). Wehling et al[9] showed that macrophages can injure normal skeletal myotubes *in vitro* and that depletion of macrophages in *mdx/mdx* mice prevents muscle necrosis, suggesting a macrophage-dependent cytotoxic activity. On the other hand, few T lymphocytes are found in skeletal muscles and heart,[10] and their role has also been largely associated with increased muscle damage. Early depletion of CD4$^+$ or CD8$^+$ T cells (at 6 to 8 days of age) led to reduced pathology.[11] Moreover, adoptive transfer of *mdx/mdx* splenocytes and muscle extract to C57BL/10 resulted in increased migration of CD8$^+$ T cells to muscle and increased pathology, but no increase in CK levels.[11] However, antibody-mediated depletion of CD4$^+$ or CD8$^+$ T cells of 4week-old *mdx/mdx* mice did not influence fibrosis in older mice.[12] Although the contribution of cytotoxic T lymphocytes to DMD pathology remains unclear,[13] experiments using null mutants for both dystrophin and perforin showed that lack of perforin decreased dystrophic muscle pathology.[14]

Supported by the Oswaldo Cruz Foundation (Fundação Oswaldo Cruz) and the National Council for Scientific and Technological Development (Conselho Nacional de Desenvolvimento Científico e Tecnológico-CNPq).

Accepted for publication April 12, 2012.

Address reprint requests to Andrea Henriques-Pons, Av. Brasil, 4365, Pavilhão Cardoso Fontes, 2° andar sala 66, Manguinhos, CEP 21040-900, Rio de Janeiro, RJ, Brazil. E-mail: andreah@ioc.fiocruz.br.

Unlike the case with DMD patients and *mdx/mdx* mice, inflammatory foci of many myopathies are composed mostly of T lymphocytes, regardless of their protective or pathological role. $CD8^+$ T cells invading non-necrotic muscle fibers are typically found in polymyositis, for example, and cellular infiltrations in dermatomyositis and inclusion body myositis consist predominantly of $CD4^+$ T lymphocytes.[15,16] Moreover, high numbers of T cells also migrate to cardiac tissue in ischemic heart disease,[17] *Trypanosoma cruzi*-induced myocarditis,[18] and other forms of infectious myocarditis, such as coxsackie B-3 and Theiler virus.[19,20] It is currently not known why few T cells are found in DMD muscles, or whether pre- or postendothelial interactions are lacking or malfunctional.

Leukocyte recruitment into inflamed tissues is a multistep cascade of adhesive interactions between leukocytes and endothelial cells.[21] This involves selectin-mediated leukocyte tethering and rolling, in which CD62E and CD62P are expressed on the activated endothelium and CD62L is constitutively expressed on leukocytes.[22] The second step is the integrin-dependent firm adhesion of leukocytes (expressing LFA-1 and VLA-4) to the endothelial layer (expressing ICAM and VCAM) and, finally, transmigration.[23] A large number of cell types express CD62L (including monocytes, T and B lymphocytes, eosinophils, NK cells, and neutrophils), and a variety of ligands have been described (including GlyCAM-1, CD34, MadCAM-1, and PSGL-1).[24,25] Integrins must undergo functional activation for efficient interaction with counter-receptors, which is mediated by chemokines and cytokines and results in increased affinity for the ligands.[26] Blood leukocyte recruitment and transmigration to tissues is essential for appropriate inflammatory responses against infection and injury.

CD62L, also known as L-selectin, is a 90-kDa glycoprotein with two basic functions: lymphocyte homing to lymph nodes during normal blood/lymph recirculation and migration of leukocytes to inflammatory sites.[27] Some authors have believed that CD62L is important to T cells homing to lymph nodes, but not to nonlymphoid tissues.[28] However, it was shown by others that CD62L also plays a role in T-cell migration to inflamed tissues.[24,29,30] The binding of CD62L to its ligands on activated endothelial cells initiates a cascade of downstream intracellular events in the leukocyte, resulting in free cytosolic calcium increase and phosphorylation of targeted proteins, including mitogen-activated protein kinases (MAPKs).[31] These intracellular events result in rapid endoproteolytic cleavage of L-selectin from the membrane proximal domain, leading to the shedding of a functionally active L-selectin to blood.[32] This L-selectin sheddase has been identified in thymocytes as the tumor necrosis factor α converting enzyme (TACE).[33] Endothelial-independent shedding of L-selectin from leukocytes can be induced by different stimuli, including phorbol myristate acetate and bacterial streptolysin O, and cross-linking with anti-L-selectin and ATP through P2X7 receptor.[34–36] Increased soluble L-selectin can alter the ability of immune cells to interact with high-endothelial venules and migration to inflamed tissues by masking the ligands on endothelial cells, leading to reduced inflammatory responses.[37]

The P2X7 receptor is a ligand-gated ion channel that mediates nonselective cation conductance when stimulated with appropriate ligands, such as extracellular ATP (ATP_e). However, prolonged exposure or high concentrations of ATP_e lead to a pore formation that renders plasma membrane permeable to molecules such as propidium iodide (PI) and YO-PRO Yellow.[38] A variety of cells express P2X7 receptor, including lymphocytes, granulocytes, osteoclasts, osteoblasts, microglia, monocytes, and macrophages,[39,40] and it is known that inflammatory cytokines (eg, TNF and IFN-γ) can up-regulate the expression of P2X7.[41] Regarding CD62L shedding induced by P2X7 activity, Sengstake et al[35] showed that agonistic stimulation of the receptor resulted in proteolytic cleavage of CD62L from both naïve and memory B and T cells. Scheuplein et al[42] showed that endogenous sources of NAD^+ and ATP released from lysed cells activate P2X7 on T lymphocytes, leading to CD62L shedding from cell surface.

Despite the strong inflammatory process evident in DMD muscles, little is known about the mechanisms governing leukocyte trafficking into these tissues. To evaluate the ability of T cells to migrate to cardiac tissue, we sought to explore the role played by adhesion molecule-mediated T cell-endothelium interactions in *mdx/mdx* mice. Our results show a defective migration of T cells to the heart of these mice, which may be, at least in part, a result of CD62L shedding from T-cell surface. Furthermore, we show that this shedding is induced by P2X7 *in vitro* and *in vivo*, because the blockage of the receptor after Brilliant Blue G (BBG) treatment led T lymphocytes in *mdx/mdx* mice to retain functional CD62L on the membrane and allowed their migration to the heart.

Materials and Methods

Animals

All experiments were conducted with mice obtained from the Center for Breeding of Laboratory Animals at Fundação Oswaldo Cruz. We used 6-, 9-, 12-, 24-, and 48-week-old male *mdx/mdx* mice and age-matched C57BL/10 control mice. Mice were housed for 7 to 10 days at the Center for Animal Experimentation under environmental factors and sanitation according to the Guide for the Care and Use of Laboratory Animals (8th edition, 2011). This project was approved by the Fiocruz Committee of Ethics in Research (0308/06), according to resolution 196/96 of the National Health Council of Brazilian Ministry of Health. To avoid possible interference from genetic and environmental drift in the mouse colony used, most experiments were repeated with C57BL/10 and *mdx/mdx* mice obtained from the Multidisciplinary Center for Biological Investigation (CEMIB/Unicamp, Sao Paulo, Brazil). This is an internationally certified animal breeding facility and a member of the International Council for Laboratory Animal Science (ICLAS). All results were reproducible using both colonies.

Isolation of Cardiac Inflammatory Cells

Hearts from *mdx/mdx* and C57BL/10 mice were collected and cut in fragments 1 to 2 mm thick in ice-cold PBS. Fragments were then transferred to a 0.1% solution of collagenase type IV (5.2 U/mg) (Sigma-Aldrich, St. Louis, MO) and submitted to four or five cycles of enzymatic digestion under gentle agitation for 20 minutes each at 37°C. Isolated cells were centrifuged and immediately transferred to ice-cold RPMI 1640 medium supplemented with 10% fetal calf serum (Sigma-Aldrich) and maintained in ice.

Flow Cytometry

For phenotypic labeling by flow cytometry, all cells were incubated for 30 minutes at 4°C with RPMI 1640 medium supplemented with 10% fetal calf serum and 10% inactivated normal sheep serum for FcγR blockage. Cells were incubated with previously titrated APC/Cy7-conjugated anti-CD3, fluorescein isothiocyanate-conjugated anti-CD4, phycoerythrin (PE)-conjugated anti-CD8, fluorescein isothiocyanate-conjugated anti-CD62L, PE/Cy7-conjugated anti-CD69, PE-conjugated anti-LFA-1 (all from eBioscience, San Diego, CA), PE-conjugated anti-CD49d (SouthernBiotech, Birmingham, AL), and/or PE-conjugated anti-CD43 (BD Pharmingen, San Diego, CA) for 30 minutes in ice. All samples were washed twice in RPMI 1640 medium and fixed using 2% formaldehyde (EMD Chemicals, Gibbstown, NJ) in PBS until acquisition in a FACSCalibur flow cytometer (BD Biosciences, San Jose, CA) or a Dako Cyan ADP analyzer (Beckman Coulter, Houston, TX). Data analysis was performed using Dako Summit version software 4.3. For cytokine secretion, we used a cytometric bead array flex set, as recommended by the manufacturer (BD Pharmingen).

Permeabilization Assay

Blood was collected by cardiac puncture in the presence of heparin and peripheral blood mononuclear cells (PBMCs) were obtained by Ficoll-Histopaque 1077 gradient (StemCell Technologies, Vancouver, BC). Cells were incubated for 30 minutes at 4°C with fluorescein isothiocyanate-conjugated anti-CD3, anti-CD4, or anti-CD8 (SouthernBiotech), washed in RPMI 1640 medium, resuspended in prewarmed RPMI 1640/HEPES 10 mmol/L for 5 minutes at 37°C, and incubated for 10 minutes in the presence or absence of ATP_e (5 mmol/L; Sigma-Aldrich). During the last 5 minutes of incubation, propidium iodide (Sigma-Aldrich) was added at the final concentration of 0.1 μg/mL, and all samples were immediately acquired in a FACSCalibur flow cytometer (BD Biosciences). Peritoneal cells were collected using ice-cold RPMI 1640/HEPES 10 mmol/L; cells in a macrophage region based on forward scatter by side scatter (FSC $\times$ SSC) were used as a positive control.

Purification of Blood T Lymphocyte Subsets

PBMCs were obtained as described above, and 1×10^7 cells were incubated with bead-conjugated anti-CD4, anti-CD8, or anti-CD3 (Miltenyi Biotec, Auburn, CA) for 20 minutes at 4°C, resuspended in 500 μL of PBS, and applied to a MiniMACS column (Miltenyi Biotec) under a magnetic field, as recommended by the manufacturer. Samples were centrifuged and resuspended in RPMI 1640 medium and sort purity was determined by labeling the cells with fluorescein isothiocyanate-conjugated anti-CD4, anti-CD8, or anti-CD3 (SouthernBiotech) for flow cytometry analysis. We used samples of $\geq$95% enrichment for T-cell subsets.

Dot Blotting

Blood samples were obtained from *mdx/mdx* or C57BL/10 mice by cardiac puncture without heparin; samples were left at room temperature for 30 minutes. Serum was obtained by blood centrifugation at 500 $\times$ *g* for 5 minutes, and protein concentration was determined using a Lowry modified RC DC protein assay (Bio-Rad Laboratories, Hercules, CA). For dot-blotting assay, serum samples with 80, 40, or 20 μg of total proteins/100 μL of Tris buffer were added per well. Proteins were then immobilized in Tris buffer prehydrated nitrocellulose membranes for 15 minutes at room temperature, blocked for 60 minutes in Tris buffer supplemented with 5% bovine serum albumin (Sigma-Aldrich), and incubated with anti-CD62L or anti-LFA-1 (eBioscience) for 1 hour at room temperature. The membrane was then washed twice with Tris buffer and incubated for 1 hour with goat anti-rabbit alkaline phosphatase-conjugated secondary antibody (SouthernBiotech). Primary antibody was suppressed in one of the samples for negative control. Detection was performed using 5-bromo-4-chloro-3-indolyl phosphate/nitro blue tetrazolium solution (BCIP/NBT; SouthernBiotech).

Western Blotting

Purified T lymphocytes were lysed, as described previously,[43] with extraction buffer (Tris-HCl 50 mmol/L, 1% NP-40, leupeptin 1 mmol/L, phenylmethylsulfonyl fluoride 100 mmol/L, pepstatin A 1 mmol/L, EDTA 100 mmol/L; all purchased from Sigma-Aldrich). Total proteins (50 μg/slot) were resolved using SDS-PAGE (12%). Proteins were then transferred to nitrocellulose membranes, blocked using nonfat dry milk (5%) in Tris buffer, and incubated with anti-P2X7 primary antibody (Alomone, Jerusalem, Israel) for 2 hours. The membrane was then rinsed in blocking buffer and incubated with goat anti-rabbit alkaline phosphatase-conjugated secondary antibody (SouthernBiotech) for 1 hour. Detection was performed using BCIP/NBT (SouthernBiotech). For TCR $\alpha\beta$ detection, a fragment of left ventriculus was extensively washed in ice-cold PBS and cut in fragments 1 to 2 mm thick. Total proteins were extracted using extraction buffer, centrifuged at 500 $\times$ *g* for 5 minutes and subjected to SDS-PAGE as described above. Nitrocellulose mem-

branes were incubated with biotin-conjugated anti-TCR $\alpha\beta$ (MyBioSource, San Diego, CA), rinsed in blocking buffer, and incubated with horseradish peroxidase-conjugated streptavidin (Dako, Carpinteria, CA) for 1 hour. Detection was performed by chemifluorescence using an ECL plus kit (GE Healthcare, Piscataway, NJ) in a Storm 860 imaging system (Amersham-GE Healthcare, Uppsala, Sweden).

In Vitro *Blockage of P2X7*

Blood $CD3^+$ T lymphocytes purified from 9-week-old *mdx/mdx* and C57BL/10 mice were preincubated or not with KN-62 (100 nmol/L) for 30 minutes and then incubated with only medium or ATP_e 100 μmol/L for 1 hour. We chose this concentration based on a kinetic study considering the lowest dose of ATP that induced CD62L shedding with no cell death or permeabilization, as ascertained by 7-aminoactinomycin D and PI, respectively (data not shown). Supernatants were collected and used in dot-blotting assays revealed with anti-CD62L and goat anti-rabbit alkaline phosphatase-conjugated secondary antibody.

Adhesion Assay

The ability of peripheral blood $CD4^+$ and $CD8^+$ T cells to attach to cardiac vessels was tested in a modified Stamper-Woodruff assay.[44] Freshly cut, unfixed, frozen cardiac sections (15 μm thick) from 6- or 24-week-old *mdx/mdx* or C57BL/10 mice were incubated with 100 μL of a cell suspension containing 3×10^6 purified CD4 or CD8 T cells from 6- or 12-week-old *mdx/mdx* mice in RPMI 1640 medium with 10 mmol/L HEPES and 5% fetal calf serum. The incubation was performed under gentle circular agitation at 60 revolutions per minute for 40 minutes at room temperature. After extensive washings with prewarmed PBS, the slides were fixed and stained with a Romanowsky-based staining kit (Laborclin, Pinhais, Brazil), according to the manufacturer's instructions. The number of adhered cells per blood vessel was counted under a light microscope. To characterize cell surface molecules involved in T-cell adhesion to endothelial cardiac blood vessels, some experiments were conducted with purified T cell subsets pretreated with different concentrations of anti-CD62L or anti-LFA-1 monoclonal antibodies (eBioscience).

BBG Treatment for in Vivo *Blockage of P2X7*

BBG reagent (Sigma-Aldrich) was diluted at 3 mg/mL in vehicle solution (calcium- and magnesium-free PBS/0.2% dimethyl sulfoxide; Sigma-Aldrich). For *in vivo* treatment, *mdx/mdx* and C57BL/10 mice were weighed once a week during drug administration and received freshly prepared BBG (45.5 mg/kg) or vehicle via intraperitoneal injection every 48 hours. Mice were treated from 9 to 12 weeks of age.

T. cruzi *Infection*

Parasites were isolated from infected Swiss-Webster mice as described previously[45] and *mdx/mdx* or C57BL/10 mice were intraperitoneally injected with 1×10^4 blood trypomastigote forms of *T. cruzi* Y strain in 200 μL of PBS. Age-matched, uninfected control mice received 200 μL of PBS and were treated under the same conditions. Samples were collected on day 15 after infection.

Histopathological Analysis

Control and infected C57BL/10 and *mdx/mdx* mice were euthanized, and the hearts were removed, sagittally divided, and fixed using Millonig-Rosman solution (10% formaldehyde in PBS). Paraffin-embedded samples were further processed and stained with H&E in 5-μm-thick slices. In *T. cruzi*-infected mice, the number of inflammatory foci (defined as $\geq$10 inflammatory cells) and the number of inflammatory cells per focus were determined by scanning the whole tissue in approximately 30 individual microscopic fields per sample.

Immunohistochemistry

Cardiac muscles were collected, frozen using cold isopentane,[46] and stored in liquid nitrogen until use. Cardiac slices (8 μm thick) were then fixed with 4% formaldehyde for 10 minutes at room temperature and then were washed twice in PBS. Endogenous peroxidase was blocked with 3% H_2O_2 for 10 minutes, and then slices were washed twice more. FcγR was blocked, and the slices were incubated with anti-CD3ε chain primary antibody (SouthernBiotech) overnight at room temperature under agitation. Slices were washed with PBS and incubated with goat anti-rat biotin-conjugated secondary antibody (Santa Cruz Biotechnology, Santa Cruz, CA) for 1 hour and then with horseradish peroxidase-conjugated streptavidin (Dako) for 1 hour. Detection was performed using 3-amino-9-ethylcarbazole (Dako).

Biochemical Analysis

CK isoforms from cardiac (CK-MB) and skeletal (CK-NAC) muscles were assessed in mouse serum. Blood samples were collected from tail snips in heparinized capillary tubes, centrifuged, and analyzed using commercially available kits (Wiener Laboratories, Rosario, Argentina). This quantitative assay is used as a marker of muscle damage; data are expressed as a rate of NADPH increase (ΔE/min) in three sequential readings in a spectrophotometer (Molecular Devices, Sunnyvale, CA) at 340 nm.

Spontaneous Mouse Activity

We used a video tracking system to measure spontaneous activity (EthoVision XT6; Noldus, Leesburg, Holland), with a recording camera placed at a distance of 1 m from the subjects. Each mouse was individually adapted in the

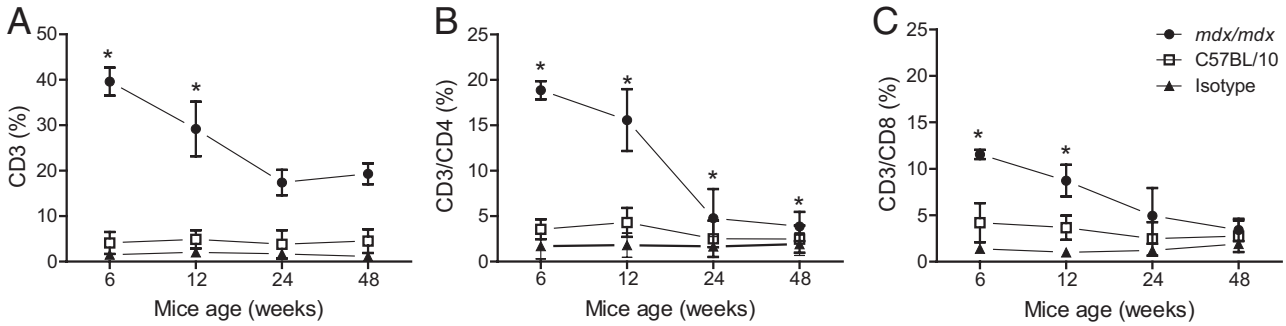

Figure 1. Distribution of T lymphocytes in cardiac tissue from *mdx/mdx* and C57BL/10 mice. Cardiac tissue was enzymatically dissociated, and all cells were obtained for flow cytometry analysis. Mononuclear cells were gated by FSC × SSC parameters and analyzed according to the expression of CD3 (**A**), CD3/CD4 (**B**), and CD3/CD8 (**C**) at 6, 12, 24, and 48 weeks of age. Data are expressed as means ± SD from five independent experiments. $^*P \leq 0.05$ versus C57BL/10. $n = 4$ or 5 animals per group.

arena for 10 minutes before the experimental measurement, which lasted 20 minutes.[47]

Statistical Analysis

Data were analyzed using Student's *t*-test (GraphPad Prism version 4.00 software; GraphPad Software, La Jolla, CA). A *P* value of ≤0.05 was considered significant.

Results

Cardiac T-Cell Numbers and CD62L Shedding to Blood

Given that most previous studies have associated T cells with increased pathology in DMD, we evaluated by flow cytometry the presence of these cells in cardiac muscles from 6-, 12-, 24-, and 48-week-old *mdx/mdx* mice (Figure 1). $CD3^+$ T cells progressively decreased in the time frame studied (Figure 1A), although with a predominance of $CD3^+/CD4^+$ T cells over $CD3^+/CD8^+$ T cells in 6- and 12-week-old animals (Figure 1, B and C). We found neither NK, NKT, nor T_{reg} cells in the cardiac muscle of *mdx/mdx* mice (data not shown), and did not find T cells at >5% in C57BL/10 mice.

Because blood T cells from *mdx/mdx* mice could be less competent to migrate to cardiac tissue, we checked the panel of adhesion molecules expressed by blood and cardiac T cells. We observed normal levels of CD62L expression in blood T lymphocytes from 6- and 12-week-old C57BL/10 mice and 6-week-old *mdx/mdx* mice. This means that very few T cells were $CD62L^-$ (Figure 2A). However, many T cells from 12-week-old *mdx/mdx* mice became $CD62L^-$ (Figure 2A). This down-regulation was transitory, because we observed that 24-week-old *mdx/mdx* mice express similar levels of selectin, compared with age-matched C57BL/10 mice (data not shown). Cardiac T lymphocytes from 6- and 12-week-old *mdx/mdx* mice expressed low levels of this molecule (Figure 2B), as expected after endothelial interaction.[22] We observed no differences in the expression of LFA-1, CD43, and CD49d in blood T cells from C57BL/10 and *mdx/mdx* mice at all ages, and there were always normal levels of CD62L expression in blood granulocytes and monocytes (data not shown). To determine whether the CD62L down-regulation could be due to cleavage from the T-cell surface, we evaluated the levels of this soluble molecule in mouse serum by dot blotting. The 12-week-old *mdx/mdx* mice had higher levels of soluble CD62L, compared with 6-week-old mice (Figure 2, C and E). LFA-1 was used as a control, and we never observed increased levels of this molecule in blood (Figure 2, D and F).

CD62L is a key molecule for naïve T cells homing to lymph nodes, where antigen interaction takes place for cell activation and effector function. However, despite the shedding of CD62L that we observed, immunosuppression has not been described in *mdx/mdx* mice, suggest-

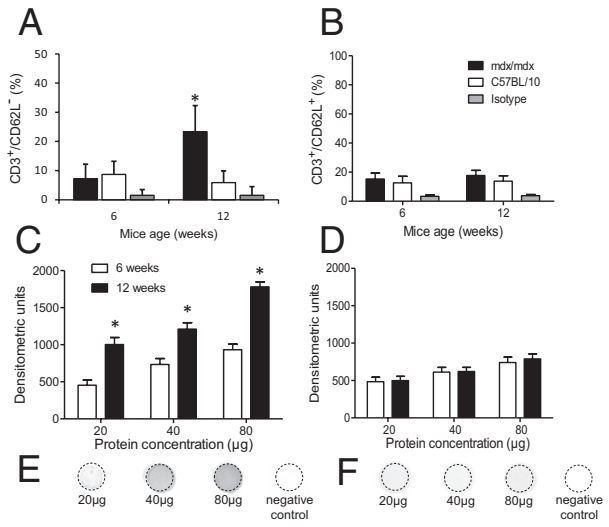

Figure 2. T-cell expression and blood soluble CD62L in *mdx/mdx* mice. PBMCs (**A**) and cardiac cells (**B**) were obtained from 6- and 12-week-old *mdx/mdx* and C57BL/10 mice and labeled with anti-CD3 and anti-CD62L. Shown is the percentage of $CD3^+/CD62L^-$ PBMCs (**A**) and $CD3^+/CD62L^+$ (**B**) or isotype labeling (**A** and **B**) as gated in the morphological region (FSC × SSC) of mononuclear cells. Serum concentrations of CD62L (**C**) and LFA-1 (**D**) in 6- and 12-week-old *mdx/mdx* mice was evaluated by dot blotting using 20, 40, and 80 μg of total proteins per slot. Representative membranes of CD62L (**E**) and LFA-1 (**F**) of 12-week-old *mdx/mdx* mice are shown. Membrane labeling was performed with primary antibody, then phosphatase alkaline-conjugated goat anti-rat secondary antibody, and revealed with NBT/BCIP. For negative control, 80 μg of total proteins were immobilized and primary antibody was omitted. Data are expressed as means ± SD from four independent experiments. $^*P \leq 0.05$. $n = 4$ or 5 animals per group.

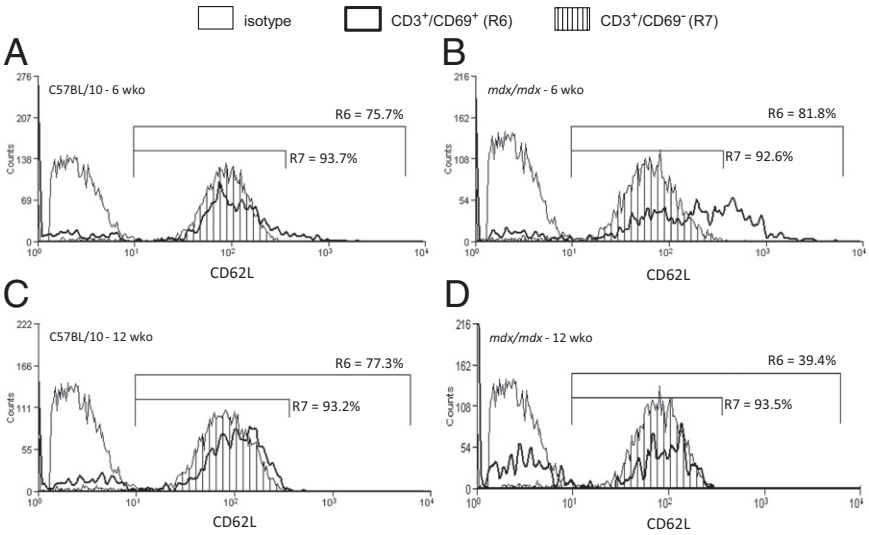

Figure 3. CD62L expression and activation status of blood T cells. PBMCs from 6- and 12-week-old C57BL/10 and *mdx/mdx* mice were labeled with anti-CD3, anti-CD69, and anti-CD62L monoclonal antibody and analyzed by flow cytometry in FSC × SSC gated PBMCs. Percentages of $CD3^+/CD69^+$ and $CD3^+/CD69^-$ cells expressing CD62L are defined by R6 and R7 markers, respectively. Data are representative of three independent experiments. $n = 3$ or 4 animals per group.

ing that naïve T-cell homing to lymph nodes is preserved. We then decided to evaluate whether the shedding of CD62L was from activated or naïve T-cell subpopulations. Using the early activation marker CD69, we found no reduction of CD62L expression in $CD69^+$ or $CD69^-$ T cells from 6-week-old C57BL/10 mice (Figure 3A), 6-week-old *mdx/mdx* mice (Figure 3B), and 12-week-old C57BL/10 mice (Figure 3C). On the other hand, although there was no down-regulation of CD62L in $CD69^-$ T cells from 12-week-old *mdx/mdx* mice (Figure 3D), only approximately 40% of $CD69^+$ T cells from these mice retained this selectin on cell surface (Figure 3D).

Limited Ability of Blood $CD62L^-$ T Cells to Firmly Adhere to Cardiac Vessels

Because the reduction of CD62L expression in blood T lymphocytes coincides with reduction of T cells in cardiac tissue, we tested the adhesion of these blood T cells to cardiac vessels *in vitro*. Purified blood $CD4^+$ or $CD8^+$ T lymphocytes from 6- or 12-week-old *mdx/mdx* mice were placed to adhere over cardiac tissue sections from 6- or 24-week-old C57BL/10 or *mdx/mdx* mice. Blood lymphocytes from 6- and 12-week-old *mdx/mdx* mice did not adhere to cardiac vessels in sections from control C57BL/10 mice (Figure 4, A and D). Likewise, T lymphocytes from 12-week-old *mdx/mdx* mice did not adhere to cardiac vessels from 6- or 24-week-old *mdx/mdx* mice, although endothelial cells were probably activated (Figure 4, B and D), because we observed inflammatory foci through H & E staining. On the other hand, blood T lymphocytes from 6-week-old *mdx/mdx* mice were capable of adhering to cardiac vessels from either 6- or 24-week-old *mdx/mdx* mice (Figure 4, C and D). We chose 24-week-old mice because the onset of tissue inflammation in the heart is present in older mice, which involves primarily macrophages. We also observed that $CD4^+$ and $CD8^+$ T cells from 6-week-old *mdx/mdx* mice preferably adhered to vessels in proximity to inflamed areas of *mdx/mdx* cardiac slices (data not shown). Moreover, we observed no differences in cardiac endothelial cell expression of VCAM and ICAM between 6- and 12-week-old *mdx/mdx* and age-matched C57BL/10 mice (data not shown). Because we found few T cells from 12-week-old

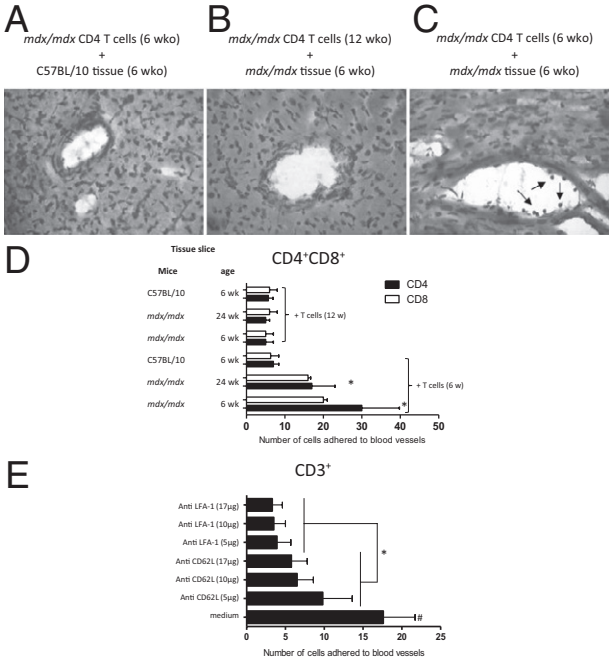

Figure 4. T lymphocytes binding to cardiac endothelium. **A–C:** $CD4^+$ T cells from *mdx/mdx* mice were purified from blood by magnetic sorting at indicated 6 or 12 weeks of age (wko) and were incubated over fresh frozen cardiac tissue slices from C57BL/10 or *mdx/mdx*. **Arrows** indicate blood purified T lymphocytes adhering to cardiac vessels. **D:** Quantification of purified $CD4^+$ or $CD8^+$ T cells adhering to cardiac blood vessels in C57BL/10 and *mdx/mdx* mice at 6 or 24 weeks of age. **E:** Blood purified $CD3^+$ T cells from 6-week-old *mdx/mdx* mice were preincubated with either medium alone or neutralizing antibodies against CD62Lor LFA-1 at three different concentrations. These cells were then incubated under agitation over fresh frozen cardiac slices from 6-week-old *mdx/mdx* mice and the number of cells adhering to cardiac blood vessels was quantified. Data are expressed as means ± SD from three independent experiments. $^*P \leq 0.05$ *mdx/mdx* versus control (**D**) or a given concentration versus preincubation with CD62L or LFA-1 (**E**); $^\dagger P \leq 0.05$ versus all other variables. $n = 5$–7 animals per group. Original magnification, ×400.

mdx/mdx mice bound to cardiac vessels (Figure 4D), we tested whether the weak adhesion might be associated with the lower levels of CD62L on T cells from these mice. Blood purified $CD4^+$ lymphocytes from 6-week-old *mdx/mdx* mice were then incubated with anti-CD62L or anti-LFA-1 before the adhesion assay. We observed that, although the blockage of LFA-1 is more efficient in impairing lymphocyte/endothelial cell interaction, the blockage of CD62L also reduces T-cell adhesion to cardiac vessels (Figure 4E). At this point, it seemed to us that there are two different pathways for CD62L shedding in 12-week-old *mdx/mdx* mice: first, normal shedding of CD62L from leukocytes, including T cells, during endothelial interaction for transmigration to inflamed tissues; second, CD62L shedding from T cells in blood, before blood vessel interaction, reducing endothelial adhesion. We therefore decided to explore possible mechanistic pathways that might be leading to the second pathway for CD62L shedding.

P2X7-Induced CD62L Shedding from Blood T Cells

Because P2X7 receptor can induce CD62L proteolytic cleavage, we evaluated the function and expression of this receptor in T cells from C57BL/10 and *mdx/mdx* mice. We first performed a permeabilization assay to evaluate P2X7 ability to induce pore formation on cell membrane on activation by ATP_e. We observed an increase in ATP_e-induced permeabilization in T lymphocytes from 6-week-old *mdx/mdx* mice, compared with 6- and 12-week-old C57BL/10 and 12-week-old *mdx/mdx* mice (Figure 5, A and B). To determine P2X7 ability to induce CD62L shedding, we performed an *in vitro* assay with purified blood T cells obtained from 9-week-old *mdx/mdx* and C57BL/10 mice incubated in the presence or absence of an antagonist of P2X7 (KN-62) and then stimulated with ATP_e. We chose the age of 9 weeks because this is when the shedding process begins (data not shown). T cells from *mdx/mdx* mice were more susceptible to ATP_e-induced CD62L shedding than C57BL/10 mice, and this shedding was blocked by KN-62 (Figure 5C). Once more, LFA-1 was used as a control and no shedding was observed (Figure 5D). We performed Western blotting to evaluate whether P2X7 expression was up-regulated in T lymphocytes from 12-week-old *mdx/mdx* mice; levels of P2X7 expression were similar in 6- and 12-week-old *mdx/mdx* and C57BL/10 mice (Figure 5E). Because IFN-γ and TNF are known to up-regulate P2X7 activity in monocytes, we evaluated whether these cytokines were increased in blood from 12-week-old *mdx/mdx* mice; however, no differences were observed between 6- and 12-week-old *mdx/mdx* mice (data not shown).

To assess the *in vivo* relevance of our findings, we treated *mdx/mdx* and C57BL/10 mice for 3 weeks with BBG, another antagonist of P2X7, and then evaluated CD62L expression on blood T lymphocytes and the concentration of soluble CD62L in serum. First, we tested whether the treatment was efficient in blocking the receptor through an ATP_e-induced permeabilization assay using peritoneal macrophages, cells that are greatly susceptible to ATP. We observed that BBG administration almost abolished ATP_e-induced pore formation in cells from both *mdx/mdx* (reduction from 77.4% to 16.2%) and C57BL/10 mice (reduction from 90.8% to 13.3%) (Figure 6, A and B). Regarding CD62L, we observed that BBG treatment restored its expression in blood T lymphocytes from *mdx/mdx* mice (increase from 35.4% to 81.1%) (Figure 6C). On the other hand, blood T cells from BBG- or vehicle-treated C57BL/10 mice were $CD62L^+$ (90.9% and 92.4%, respectively) (Figure 6D), although with a higher frequency of CD62L expression in vehicle-treated (MFI = 70), compared with BBG-treated mice (MFI = 32). Simultaneously, BBG treatment reduced soluble levels of CD62L only in blood from *mdx/mdx* mice (Figure 6, E and G).

We then decided to evaluate whether, after BBG treatment, more T cells would be able to reach the cardiac tissue of these mice. We performed Western blotting assays with cardiac extracts from BBG- and vehicle-treated *mdx/mdx* and C57BL/10 mice using anti-TCR $\alpha\beta$ and observed that, after BBG treatment, T cells migrated more to the cardiac muscle of *mdx/mdx* mice (Figure 6F). Moreover, we monitored a group of mice for 5 weeks during and after BBG treatment, measuring muscle damage markers for cardiac muscle (CK-MB) (Figure 7A) and

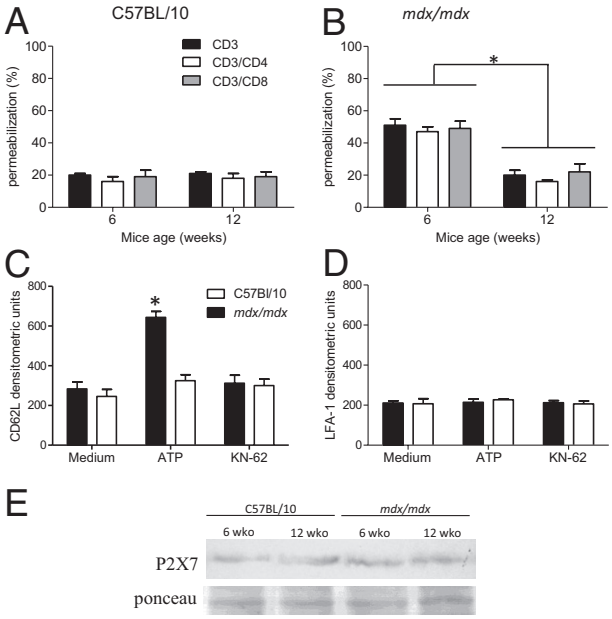

Figure 5. *In vitro* P2X7 activity in blood T cells. **A** and **B:** PBMCs from 6- and 12-week-old C57BL/10 (**A**) and *mdx/mdx* (**B**) mice were labeled with anti-CD3, anti-CD4, and anti-CD8 monoclonal antibody and incubated with ATP_e (5 mmol/L) for 10 minutes in the presence of PI in the last 5 minutes. T-cell membrane permeabilization was then evaluated by PI incorporation using flow cytometry. **C** and **D:** P2X7 ability to induce CD62L and LFA-1 shedding from purified $CD3^+$ T lymphocyte surface was evaluated by dot blotting. Purified blood $CD3^+$ T lymphocytes from 9-week-old *mdx/mdx* or C57BL/10 mice were incubated either in the presence or absence of KN-62 (a P2X7 blocker) and then stimulated with ATP_e (100 μmol/L). Supernatants were collected and used to determine CD62L (**C**) and LFA1 (**D**) levels. **E:** P2X7 expression by $CD3^+$ T lymphocytes purified from 6- and 12-week-old *mdx/mdx* and C57BL/10 mice was evaluated by Western blotting. Ponceau red staining served as control for total protein applied in each sample. Each experiment was performed three times. $^*P < 0.05$. n = 5–7 animals per group.

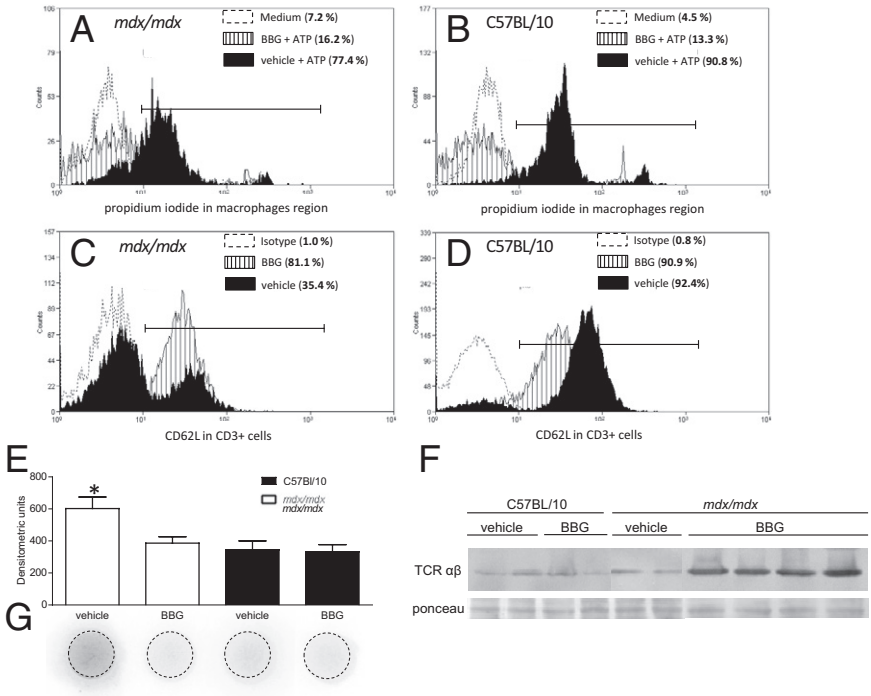

Figure 6. *In vivo* role of P2X7 in CD62L shedding from the T-cell surface. **A** and **B:** Peritoneal cells from *mdx/mdx* (**A**) and C57BL/10 (**B**) mice treated with BBG (45.5 mg/kg) or vehicle (from 9 to 12 weeks of age) were collected and incubated with ATP_e (5 mmol/L) and PI for permeabilization assays by flow cytometry in gated macrophages (FSC × SSC). Percentage of PI positive cells is indicated in parentheses. **C** and **D:** PBMCs were collected from *mdx/mdx* mice (**C**) and C57BL/10 mice (**D**) treated with BBG or vehicle. Percentage of $CD3^+/CD62L^+$ cells is indicated in parentheses. **Horizontal bars** define fluorescence positivity. **E** and **G:** Soluble CD62L was evaluated in serum samples from all groups of mice using dot-blotting assays. **F:** Cardiac tissue extracts were used for $\alpha\beta$ T-cell detection by Western blotting. Data are representative of at least three independent experiments. $^*P \leq 0.05$. $n = 4$ or 5 animals per group.

skeletal muscle (CK-NAC) (Figure 7B). BBG-treated *mdx/mdx* mice exhibited higher CK-MB and CK-NAC activity until 2 weeks of treatment, compared with all other groups; after 2 weeks, CK-NAC activity decreased, reaching levels similar to those observed in vehicle-treated *mdx/mdx* mice.

To determine whether the increase in muscle lesion observed after BBG treatment was due to increased physical activity, we evaluated motor spontaneous activity using an EthoVision video tracking system and observed that BBG-treated *mdx/mdx* mice have even lower spontaneous activity, compared with vehicle-treated *mdx/mdx* mice (Figure 7C).

Because *T. cruzi* infection induces a myocarditis composed mostly of $CD8^+$ T cells, we infected 6- and 12-week-old *mdx/mdx* mice to test whether fewer blood $CD62L^+$ T cells would lead to nonlymphoid inflammatory infiltrates. The 6- and 12-week-old infected *mdx/mdx* and C57BL/10 mice had equivalent numbers of cardiac infiltrates per field, and the numbers were higher, compared with noninfected *mdx/mdx* mice (Figure 8A). The number of inflammatory cells per inflammatory focus in infected *mdx/mdx* mice was higher than in noninfected *mdx/mdx* and infected C57BL/10 mice (Figure 8B). H&E staining of cardiac samples from 12-week-old uninfected (Figure 8C) and infected (Figure 8D) *mdx/mdx* mice showed a general appearance of inflammatory infiltration. Regarding the presence of T cells, we did not observe inflammatory infiltration and CD3 labeling in noninfected C57BL/10 mice (Figure 8E). On the other hand, cardiac tissues from infected C57BL/10 mice showed high numbers of $CD3^+$ T cells (Figure 8F), in contrast to noninfected and infected 12-week-old *mdx/mdx* mice, which have few $CD3^+$ cells (Figure 8, G and H). TCR $\alpha\beta$ stain-

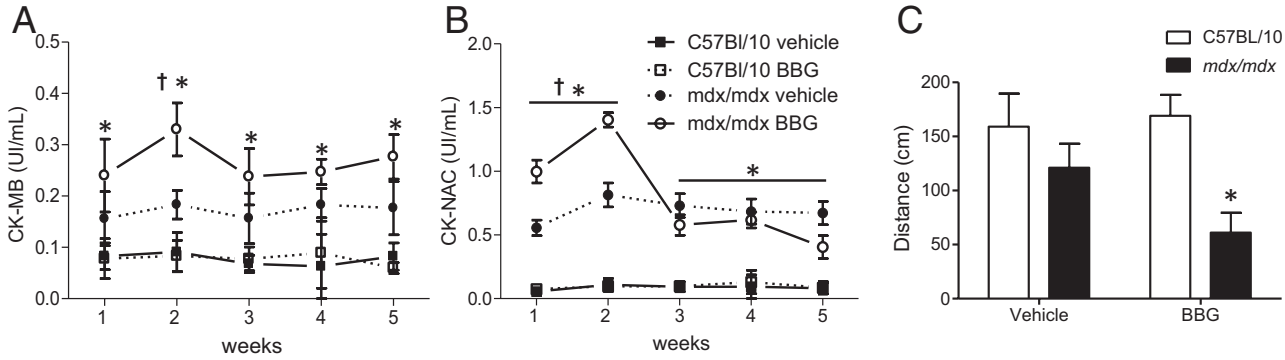

Figure 7. Analysis of muscle damage and motor activity with BBG treatment. **A** and **B:** *mdx/mdx* and C57BL/10 mice were treated with BBG (45.5 mg/kg) or vehicle from 9 to 12 weeks of age (weeks 1 to 3) and CK-MB (**A**) and CK-NAC (**B**) were measured once a week during the treatment and for 2 weeks more after the treatment (weeks 4 and 5). **C:** Motor spontaneous activity was evaluated on the second week of treatment, using a Noldus EthoVision XT6 video tracking system. $^*P \leq 0.05$ *mdx/mdx* versus treatment-matched C57BL/10 mice; $^\dagger P \leq 0.05$ treated versus untreated *mdx/mdx* mice.

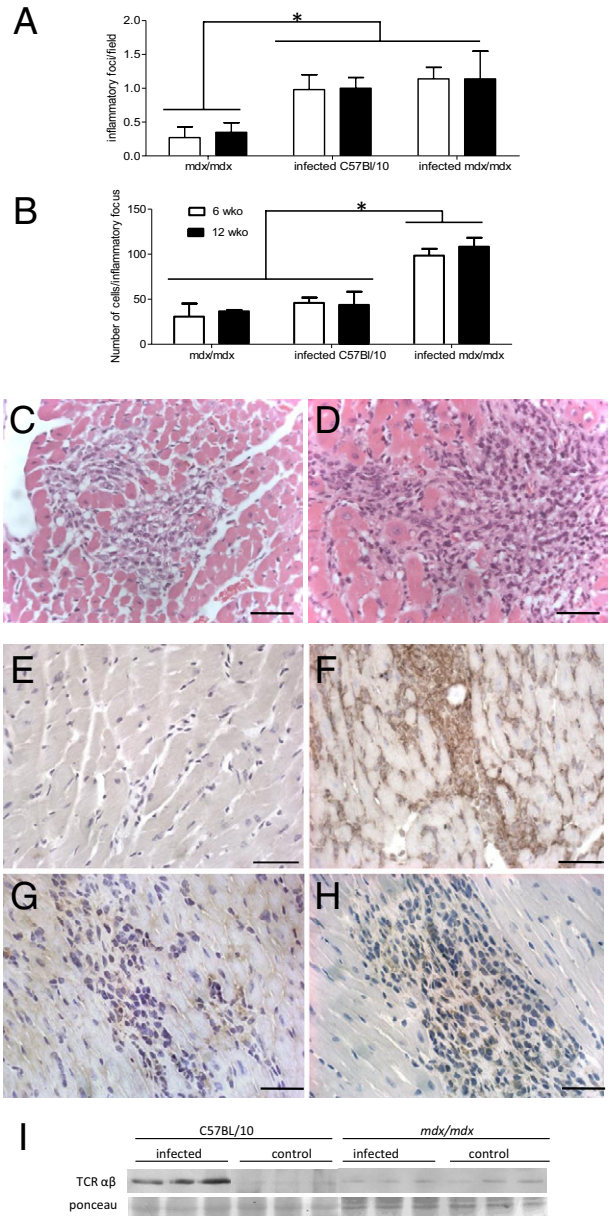

Figure 8. *T. cruzi* infection of *mdx/mdx* mice. **A** and **B:** C57BL/10 and *mdx/mdx* mice were infected with *T. cruzi* and hearts were collected 15 days after infection. The number of imflammatory foci per microscopic field (**A**) and the number of cells per inflammatory focus (**B**) were quantified by light microscopy in H&E-stained slices from 6- and 12-week-old mice. **C** and **D:** H&E-stained samples from 12-week-old uninfected (**C**) and infected (**D**) *mdx/mdx* mice were used to illustrate general characteristics of inflammatory foci. **E–H:** Identification of T cells was performed in heart slices using anti-CD3 monoclonal antibody in 12-week-old uninfected (**E**) and infected (**F**) C57BL/10 mice and in uninfected (**G**) and infected (**H**) *mdx/mdx* mice. **I:** Cardiac extracts from 12-week-old mice were used in Western blotting to evaluate T-cell lymphocytic infiltration; membranes were incubated with anti-$\alpha\beta$ TCR monoclonal antibody. **Arrows** indicate $CD3^+$ cells. $^*P \leq 0.05$. Scale bar = 50 μm.

ing in Western blotting of cardiac extracts from infected and noninfected 12-week-old *mdx/mdx* and C57BL/10 mice confirmed these data (Figure 8I). Regardless of the technique used, throughout our study we always found more cardiac T cells in control *mdx/mdx* mice, compared with control C57BL/10 mice.

Discussion

Although skeletal muscles are more studied in DMD, cardiac function and anatomy are also affected, in both patients and experimental models. Using echocardiography, Quinlan et al[48] found that 8-week-old *mdx/mdx* mice had normal cardiac function, but 29-week-old mice exhibited minor alterations and 42-week-old mice exhibited dilated cardiomyopathy; they also found a four-fold increase in interstitial cardiac fibrosis in 17-week-old *mdx/mdx* mice. Moreover, Nakamura et al[49] found an increase in left ventricular wall with inflammation and fibrosis after regular treadmill exercise. Nonetheless, the precise role of the inflammatory response to the onset of cardiac pathology is currently unknown, especially the reason why T lymphocytes are rarely found in cardiac muscle. Many reports have described a great number of myeloid cells, mainly macrophages, mast cells, and some eosinophils in cardiac and skeletal muscles.[50–52] In contrast to DMD, other myopathies (including polymyositis, inclusion body myositis, dermatomyositis, and cardiomyopathies induced by the protozoan *T. cruzi* and coxsackie B3 virus) induce migration of T lymphocytes.[15,18]

We observed that T cells, mainly $CD4^+$ T cells, are present in the cardiac tissue of 6-week-old *mdx/mdx* mice and that their frequency decreases with age, being almost undetectable in 24-week-old animals. Thus, reduced cardiac function and increased damage in older mice seem to be T cell-independent or likely delayed from early T-cell function.

Different possibilities might account for the reduced number of T cells in muscles from DMD patients and *mdx/mdx* mice, such as high levels of lymphocyte death in the tissue. This finding could be due to either cytotoxic activity of other cells targeting T lymphocytes or high production of soluble factors, such as TNF. However, we (data not shown) observed that cardiac muscles have few TUNEL-positive cells, suggesting low levels of apoptosis in the muscle, including T cells. On the other hand, the paucity of TUNEL-positive cells could be due to a very efficient scavenging process of dying cells. This can be illustrated by the presence of very few TUNEL-positive cells in thymus, despite the death of approximately 95% of thymocytes not rescued by positive selection (death by neglect) and during negative selection. Therefore, at this point and regardless of our present results, we cannot exclude the possibility that apoptosis undetected by current techniques could be occurring in cardiac muscle and contributing more or less to the reduced number of T cells.

Another possibility is inefficient migration of blood T cells to the cardiac tissue, which could be due to defective activation in lymph nodes, reduced muscle production of T cell chemotactic factors, reduced expression of chemotactic receptors by T cells, or inefficient T lymphocyte/endothelial cell interaction due to reduced expression/activation of adhesion molecules, such as selectins and integrins. Many of these alternatives remain to be tested. However, regarding the first possibility, *mdx/mdx* mice are not considered more susceptible to infections, for example, nor do they show any other characteristic of

significant reduced immunocompetence. In accord, we observed no difference in blood parasitemia after *T. cruzi* infection between *mdx/mdx* and C57BL/10 mice (data not shown). Moreover, we observed no significant differences in total $CD44^{high}$ blood T cells between 6-week-old (5.38% ± 1.17) and 12-week-old (4.54% ± 0.96) *mdx/mdx* mice. Regarding the production of TNF, IL-6, IFN-γ, IL-10, MCP-1, and IL-12 (potential regulators for T-cell migration) in extracts of reperfused hearts, we observed no significant differences between 6- and 12-week-old *mdx/mdx* mice (data not shown). On the other hand, of the various adhesion molecules for endothelial interaction (CD62L, CD49d, LFA-1, ICAM, and VCAM), only CD62L was absent from blood T cells in a window of time in *mdx/mdx* mice (10 to 20 weeks old). The 24-week-old *mdx/mdx* mice recovered expression of CD62L on T lymphocytes, although these cells were still not observed in the cardiac tissue. This suggests that CD62L-independent mechanisms can still prevent T-cell migration at this age, but this alternative remains to be tested.

Our data also showed that naïve and long-term activated T cells ($CD69^-$) retain CD62L on cell surface, and only a part of the early-activated T cells ($CD69^+$) shed the selectin. These data further support the concept that lack of CD62L in T-cell subpopulations does not affect the acquired immune response to most antigens.

CD62L down-regulation could be a result of reduced molecular transcription or translation, with membrane molecules targeted to lysosomal destruction or shedding. Because we observed high levels of serum CD62L in 12-week-old *mdx/mdx* mice, we considered proteolytic cleavage from the cell surface as the most likely alternative. Data from the literature[24,29] and our present results show that CD62L is required for T-cell migration to nonlymphoid tissues, although we and others have observed that LFA-1 seems to be more important.[23] Studies using $CD62L^{-/-}$ mice showed that leukocytes, including T cells, have significantly reduced ability to roll and enter sites of inflammation, which blunts inflammatory responses.[53] Moreover, anti-CD62L antibody administration suppressed clinical signs and T-lymphocyte infiltration in the central nervous system in an experimental autoimmune encephalomyelitis model.[54] Based on studies using a septic shock model, Chalaris et al[55] also proposed that rapid CD62L endoproteolytic release from T-cell surface modulates lymphocyte ability to migrate and enter sites of inflammation. These data further support that CD62L is necessary for T-cell rolling along the endothelium of blood vessels and for subsequent migration.

Our *in vitro* and *in vivo* results show that P2X7 activity led to CD62L shedding in 12-week-old *mdx/mdx* mice. On the other hand, although C57BL/10 and *mdx/mdx* mice expressed similar levels of P2X7, ATP_e-induced membrane permeabilization was increased only in 6-week-old *mdx/mdx* mice. We expected a different result, that permeabilization would be increased also in 12-week-old *mdx/mdx* mice, concomitant with P2X7-induced CD62L shedding. However, this is not the first finding of receptor expression, intracellular biochemical pathways, and resultant cellular responses independently triggered by P2X7 agonistic stimuli. For example, we observed previously that both *T. cruzi*-infected and noninfected C57BL/6 thymocytes expressed P2X7, but agonistic stimulus did not induce a Ca^{2+} signal or permeabilization in control mice, which acquired these functions only after infection.[43] In *mdx/mdx* mice, Young et al[56] found increased expression of P2X7 in dystrophic skeletal muscles, concomitant with higher levels of phospho-ERK1/2 and calcium influx induced by ATP_e; however, sustained activation of P2X7 by ATP_e did not induce pore formation in these cells. Together, these data show that pore formation and other P2X7 signaling pathways can be dissociated.

BBG treatment was efficient in blocking P2X7-dependent CD62L shedding and membrane permeabilization. In terms of an *in vivo* treatment, however, we do not know other possible activities of BBG over P2X7 function in other cell types, such as macrophages and mast cells that migrate to muscles, and even over other P2 receptor-dependent pathways. Regarding T cells, sustained expression of CD62L allowed cell migration to cardiac muscle and induced cardiac and skeletal lesions for 2 weeks after BBG treatment, as ascertained by CK-NAC and CK-MB. These data are in agreement with other studies showing that T cells increase pathology[11,12,14] and corroborate the importance of P2X7 and selectins to T cell-dependent muscle damage in DMD. However, we do not know whether the treatment also affected other cell types, inducing increased migration of other leukocyte subpopulations to the muscles, which could lead to more tissue damage. Nonetheless, after 3 weeks of treatment, when the mice were 12 weeks of age, we found no differences in CK levels between BBG-treated and untreated *mdx/mdx* mice, despite the migration of more T cells to the heart. This lack of difference may be due to a reduced functional effector activity of T cells, because we found that <10% of harvested cardiac T cells from 12-week-old *mdx/mdx* mice retain CD2 and $CD44^{high}$ on cell membrane, unlike 6-week-old mice, which showed higher levels of both molecules (data not shown).

To our knowledge, *mdx/mdx* mice were the first experimental model of *T. cruzi* infection that induced a nonlymphocytic myocarditis. C57BL/10 infected mice, as well as Chagas' disease patients and other experimental models, have inflammatory foci composed mostly of $CD8^+$ T lymphocytes.[57] Although it is still not completely known which cytotoxic pathways and cells induce cardiomyocyte death in the infection, it is largely accepted that T cells are mainly responsible for cell death and inflammation. In 12-week-old *mdx/mdx* mice, however, T cell competence to interact with endothelial cells is apparently so inefficient that, even after infection, most of these cells were still not able to reach the muscle. Even though the infection induced a new assortment of alterations in the immune system of *mdx/mdx* mice, it is noteworthy that T-cell migration to damaged muscles was actively prevented.

The present findings suggest that blood T cells from 12-week-old *mdx/mdx* mice lack the necessary repertoire of adhesion molecules, which may be, at least in part,

responsible for the paucity of T cells found in muscles of *mdx/mdx* mice.

Acknowledgments

We thank Marcelo Meuser Batista for infection of the mice and Dr. Robson Coutinho Silva for Western blotting support.

References

1. Muntoni F, Torelli S, Ferlini A: Dystrophin and mutations: one gene, several proteins, multiple phenotypes. Lancet Neurol 2003, 2:731–740
2. Ehmsen J, Poon E, Davies K: The dystrophin-associated protein complex. J Cell Sci 2002, 115:2801–2803
3. Waite A, Tinsley CL, Locke M, Blake DJ: The neurobiology of the dystrophin-associated glycoprotein complex. Ann Med 2009, 41:344–359
4. Fayssoil A, Orlikowski D, Nardi O, Annane D: Atteintes cardiaques au cours de la myopathie de Duchenne [Cardiac involvement in Duchenne muscular dystrophy]. Presse Med 2008, 37:648–653
5. Fukunaga H, Sonoda Y, Atsuchi H, Osame M: [Respiratory failure and its care in Duchenne muscular dystrophy]. Rinsho Shinkeigaku 1991, 31:154–158
6. Bulfield G, Siller WG, Wight PA, Moore KJ: X chromosome-linked muscular dystrophy (mdx) in the mouse. Proc Natl Acad Sci USA 1984, 81:1189–1192
7. Claflin DR, Brooks SV: Direct observation of failing fibers in muscles of dystrophic mice provides mechanistic insight into muscular dystrophy. Am J Physiol Cell Physiol 2008, 294:C651–C658
8. Deconinck N, Dan B: Pathophysiology of Duchenne muscular dystrophy: current hypotheses. Pediatr Neurol 2007, 36:1–7
9. Wehling M, Spencer MJ, Tidball JG: A nitric oxide synthase transgene ameliorates muscular dystrophy in mdx mice. J Cell Biol 2001, 155:123–131
10. Vetrone SA, Montecino-Rodriguez E, Kudryashova E, Kramerova I, Hoffman EP, Liu SD, Miceli MC, Spencer MJ: Osteopontin promotes fibrosis in dystrophic mouse muscle by modulating immune cell subsets and intramuscular TGF-beta. J Clin Invest 2009, 119:1583–1594
11. Spencer MJ, Montecino-Rodriguez E, Dorshkind K, Tidball JG: Helper (CD4(+)) and cytotoxic (CD8(+)) T cells promote the pathology of dystrophin-deficient muscle. Clin Immunol 2001, 98:235–243
12. Morrison J, Palmer DB, Cobbold S, Partridge T, Bou-Gharios G: Effects of T-lymphocyte depletion on muscle fibrosis in the mdx mouse. Am J Pathol 2005, 166:1701–1710
13. Mantegazza R, Andreetta F, Bernasconi P, Baggi F, Oksenberg JR, Simoncini O, Mora M, Cornelio F, Steinman L: Analysis of T cell receptor repertoire of muscle-infiltrating T lymphocytes in polymyositis. Restricted V alpha/beta rearrangements may indicate antigen-driven selection. J Clin Invest 1993, 91:2880–2886
14. Spencer MJ, Walsh CM, Dorshkind KA, Rodriguez EM, Tidball JG: Myonuclear apoptosis in dystrophic mdx muscle occurs by perforin-mediated cytotoxicity. J Clin Invest 1997, 99:2745–2751
15. Dalakas MC: Review An update on inflammatory and autoimmune myopathies. Neuropathol Appl Neurobiol 2011, 37:226–242
16. Fasth AE, Dastmalchi M, Rahbar A, Salomonsson S, Pandya JM, Lindroos E, Nennesmo I, Malmberg KJ, Söderberg-Nauclér C, Trollmo C, Lundberg IE, Malmström V: T cell infiltrates in the muscles of patients with dermatomyositis and polymyositis are dominated by CD28null T cells. J Immunol 2009, 183:4792–4799
17. Zuidema MY, Zhang C: Ischemia/reperfusion injury: the role of immune cells. World J Cardiol 2010, 2:325–332
18. de Oliveira GM, Diniz RL, Batista W, Batista MM, Bani Correa C, de Araújo-Jorge TC, Henriques-Pons A: Fas ligand-dependent inflammatory regulation in acute myocarditis induced by Trypanosoma cruzi infection. Am J Pathol 2007, 171:79–86
19. Gómez RM, Rinehart JE, Wollmann R, Roos RP: Theiler's murine encephalomyelitis virus-induced cardiac and skeletal muscle disease. J Virol 1996, 70:8926–8933
20. Huber SA, Job LP: Cellular immune mechanisms in Coxsackievirus group B, type 3 induced myocarditis in Balb/C mice. Adv Exp Med Biol 1983, 161:491–508
21. Carlos TM, Harlan JM: Leukocyte-endothelial adhesion molecules. Blood 1994, 84:2068–2101
22. Langer HF, Chavakis T: Leukocyte-endothelial interactions in inflammation. J Cell Mol Med 2009, 13:1211–1220
23. Denucci CC, Mitchell JS, Shimizu Y: Integrin function in T-cell homing to lymphoid and nonlymphoid sites: getting there and staying there. Crit Rev Immunol 2009, 29:87–109
24. Hickey MJ, Forster M, Mitchell D, Kaur J, De Caigny C, Kubes P: L-selectin facilitates emigration and extravascular locomotion of leukocytes during acute inflammatory responses in vivo. J Immunol 2000, 165:7164–7170
25. Rosen SD: Ligands for L-selectin: homing, inflammation, and beyond. Annu Rev Immunol 2004, 22:129–156
26. Laudanna C, Bolomini-Vittori M: Integrin activation in the immune system. Wiley Interdiscip Rev Syst Biol Med 2009, 1:116–127
27. Ley K, Kansas GS: Selectins in T-cell recruitment to non-lymphoid tissues and sites of inflammation. Nat Rev 2004, 4:325–335
28. Ager A: Regulation of lymphocyte migration into lymph nodes by high endothelial venules. Biochem Soc Trans 1997, 25:421–428
29. Grailer JJ, Kodera M, Steeber DA: L-selectin: role in regulating homeostasis and cutaneous inflammation. J Dermatol Sci 2009, 56:141–147
30. Uchimura K, Rosen SD: Sulfated L-selectin ligands as a therapeutic target in chronic inflammation. Trends Immunol 2006, 27:559–565
31. Brenner B, Gulbins E, Schlottmann K, Koppenhoefer U, Busch GL, Walzog B, Steinhausen M, Coggeshall KM, Linderkamp O, Lang F: L-selectin activates the Ras pathway via the tyrosine kinase p56lck. Proc Natl Acad Sci USA 1996, 93:15376–15381
32. Kahn J, Ingraham RH, Shirley F, Migaki GI, Kishimoto TK: Membrane proximal cleavage of L-selectin: identification of the cleavage site and a 6-kD transmembrane peptide fragment of L-selectin. J Cell Biol 1994, 125:461–470
33. Killock DJ, Ivetić A: The cytoplasmic domains of TNFalpha-converting enzyme (TACE/ADAM17) and L-selectin are regulated differently by p38 MAPK and PKC to promote ectodomain shedding. Biochem J 2010, 428:293–304
34. Jung TM, Dailey MO: Rapid modulation of homing receptors (gp90MEL-14) induced by activators of protein kinase C. Receptor shedding due to accelerated proteolytic cleavage at the cell surface. J Immunol 1990, 144:3130–3136
35. Sengstake S, Boneberg EM, Illges H: CD21 and CD62L shedding are both inducible via P2X7Rs. Int Immunol 2006, 18:1171–1178
36. Stoddart JH Jr, Jasuja RR, Sikorski MA, von Andrian UH, Mier JW: Protease-resistant L-selectin mutants. Down-modulation by cross-linking but not cellular activation. J Immunol 1996, 157:5653–5659
37. Tu L, Poe JC, Kadono T, Venturi GM, Bullard DC, Tedder TF, Steeber DA: A functional role for circulating mouse L-selectin in regulating leukocyte/endothelial cell interactions in vivo. J Immunol 2002, 169:2034–2043
38. Surprenant A, Rassendren F, Kawashima E, North RA, Buell G: The cytolytic P2Z receptor for extracellular ATP identified as a P2X receptor (P2X7). Science 1996, 272:735–738
39. Coutinho-Silva R, Persechini PM: P2Z purinoceptor-associated pores induced by extracellular ATP in macrophages and J774 cells. Am J Physiol 1997, 273:C1793–C1800
40. Wiley JS, Gargett CE, Zhang W, Snook MB, Jamieson GP: Partial agonists and antagonists reveal a second permeability state of human lymphocyte P2Z/P2X7 channel. Am J Physiol 1998, 275:C1224–C1231
41. Humphreys BD, Dubyak GR: Modulation of P2X7 nucleotide receptor expression by pro- and anti-inflammatory stimuli in THP-1 monocytes. J Leukoc Biol 1998, 64:265–273
42. Scheuplein F, Schwarz N, Adriouch S, Krebs C, Bannas P, Rissiek B, Seman M, Haag F, Koch-Nolte F: NAD+ and ATP released from injured cells induce P2X7-dependent shedding of CD62L and externalization of phosphatidylserine by murine T cells. J Immunol 2009, 182:2898–2908
43. Cascabulho CM, Menna-Barreto RF, Coutinho-Silva R, Persechini PM, Henriques-Pons A: P2X7 modulatory web in Trypanosoma cruzi infection. Parasitol Res 2008, 103:829–838

44. Stamper HB Jr, Woodruff JJ: Lymphocyte homing into lymph nodes: in vitro demonstration of the selective affinity of recirculating lymphocytes for high-endothelial venules. J Exp Med 1976, 144:828–833
45. Araújo-Jorge TC, Sampaio EP, De Souza W, Meirelles Mde N: Trypanosoma cruzi: the effect of variations in experimental conditions on the levels of macrophage infection in vitro. Parasitol Res 1989, 75:257–263
46. Guerron AD, Rawat R, Sali A, Spurney CF, Pistilli E, Cha HJ, Pandey GS, Gernapudi R, Francia D, Farajian V, Escolar DM, Bossi L, Becker M, Zerr P, de la Porte S, Gordish-Dressman H, Partridge T, Hoffman EP, Nagaraju K: Functional and molecular effects of arginine butyrate and prednisone on muscle and heart in the mdx mouse model of Duchenne muscular dystrophy. PLoS One 2010, 5:e11220
47. Haba R, Shintani N, Onaka Y, Wang H, Takenaga R, Hayata A, Baba A, Hashimoto H: Lipopolysaccharide affects exploratory behaviors toward novel objects by impairing cognition and/or motivation in mice: possible role of activation of the central amygdala. Behav Brain Res 2012, 228:423–431
48. Quinlan JG, Hahn HS, Wong BL, Lorenz JN, Wenisch AS, Levin LS: Evolution of the mdx mouse cardiomyopathy: physiological and morphological findings. Neuromuscul Disord 2004, 14:491–496
49. Nakamura A, Yoshida K, Takeda S, Dohi N, Ikeda S: Progression of dystrophic features and activation of mitogen-activated protein kinases and calcineurin by physical exercise, in hearts of mdx mice. FEBS Lett 2002, 520:18–24
50. Cai B, Spencer MJ, Nakamura G, Tseng-Ong L, Tidball JG: Eosinophilia of dystrophin-deficient muscle is promoted by perforin-mediated cytotoxicity by T cell effectors. Am J Pathol 2000, 156:1789–1796
51. Gorospe JR, Nishikawa BK, Hoffman EP: Recruitment of mast cells to muscle after mild damage. J Neurol Sci 1996, 135:10–17
52. Villalta SA, Rinaldi C, Deng B, Liu G, Fedor B, Tidball JG: Interleukin-10 reduces the pathology of mdx muscular dystrophy by deactivating M1 macrophages and modulating macrophage phenotype. Hum Mol Genet 2011, 20:790–805
53. Tedder TF, Steeber DA, Pizcueta P: L-selectin-deficient mice have impaired leukocyte recruitment into inflammatory sites. J Exp Med 1995, 181:2259–2264
54. Archelos JJ, Jung S, Rinner W, Lassmann H, Miyasaka M, Hartung HP: Role of the leukocyte-adhesion molecule L-selectin in experimental autoimmune encephalomyelitis. J Neurol Sci 1998, 159:127–134
55. Chalaris A, Adam N, Sina C, Rosenstiel P, Lehmann-Koch J, Schirmacher P, Hartmann D, Cichy J, Gavrilova O, Schreiber S, Jostock T, Matthews V, Häsler R, Becker C, Neurath MF, Reiss K, Saftig P, Scheller J, Rose-John S: Critical role of the disintegrin metalloprotease ADAM17 for intestinal inflammation and regeneration in mice. J Exp Med 2010, 207:1617–1624
56. Young C, Brutkowski W, Lien CF, Arkle S, Lochmüller H, Zabłocki K, Górecki DC: P2X7 purinoceptor alterations in dystrophic mdx mouse muscles: Relationship to pathology and potential target for treatment. J Cell Mol Med 2012, 16:1026–1037
57. Henriques-Pons A, Oliveira GM, Paiva MM, Correa AF, Batista MM, Bisaggio RC, Liu CC, Cotta-De-Almeida V, Coutinho CM, Persechini PM, Araujo-Jorge TC: Evidence for a perforin-mediated mechanism controlling cardiac inflammation in Trypanosoma cruzi infection. Int J Exp Pathol 2002, 83:67–79